DYNAMIC SPREADING AND ABSORPTION OF IMPACTING DROPLETS ON TOPOGRAPHICALLY IRREGULAR POROUS SUBSTRATES

Parvez Alam (*), Martti Toivakka (*), Kaj Backfolk (**) and Petri Sirviö (**)

(*) Laboratory of Paper Coating and Converting
Department of Chemical Engineering, Åbo Akademi University, Turku, Finland

(**) Stora Enso Oyj
Helsinki, Finland

Presented at the 13th International Coating Science and Technology Symposium, September 10-13, 2006, Denver, Colorado[1]

Introduction

Understanding the distribution profile of droplets impacted onto porous media as they simultaneously spread and absorb is paramount in coating science and engineering. Computational models of spreading or imbibing droplets have largely focused on flat surface profiles, though more recent models have also included topographical irregularity [e.g. 1, 2]. The research presented herein studies the combined influences of high impaction rates, surface energetics and surface geometries on the spreading-absorption behaviour of Newtonian fluid droplets on topographically irregular porous substrates. Irregular surface profiles were generated using quasi-random geometry location algorithms comprising hemispherical, cubic and plate-like protrusions from an initially flat surface. Simulations are also carried out using flat porous substrates. The geometries generated were used in conjunction with computational fluid dynamics software FLOW3D to conduct the fluid flow simulations. Droplet spreading and absorption can be divided into two phases. The first phase comprises an initial coupled spreading-absorption distribution, whilst the second phase is absorption dominated flow with little or no further spreading. This work focuses on the first phase characteristics. Constants that are used throughout the simulations only differ when referred to elsewhere. These constants include; fluid viscosity = 0.001Pas, contact angle = 30^{o}, surface tension coefficient = $50mNm^{-1}$, porous media capillary pressure = 90 000Pa, porous media porosity = 30%, porous media drag coefficients = 2.5×10^{6} and 1.8×10^{14}.

Flat substrates – effect of droplet size, impact speed and viscosity

Initial simulations were carried out on flat porous substrates to ascertain the generic effects of droplet size and impaction rates on the characteristics of droplet spreading and absorption. When the normalised droplet spread, d*, is plotted against the maximum depth of absorption, ζ, for different droplet sizes and speeds, d* is seen to increase exponentially with the depth of absorption. The magnitude of spreading and absorption also rises with an increasing droplet size. At $1ms^{-1}$, significantly more absorption and less spreading occurs than for $25ms^{-1}$ impacting droplets, where the impaction rate generates higher spreading profiles. At $50ms^{-1}$ however, absorption is higher than for $25ms^{-1}$ impact velocities. When the pressure profiles are checked at the interface of the droplet and the substrate material, it is found that at impact velocities of $25ms^{-1}$, the maximum interfacial pressures generated are *c.a.* 59kPa, whereas, at $50ms^{-1}$ the interfacial pressures are 1.157MPa. It is postulated that spreading will increase and absorption will decrease as the impact velocity rises, until the interfacial pressures exceed the capillary pressure. After the interfacial pressures exceed the capillary pressure, absorption will once again increase under the influence of external pressures that drive the fluid into the porous media.

---

[1] Unpublished. ISCST shall not be responsible for statements or opinions contained in papers or printed in its publications.

Simulations carried out where the droplet viscosity, μ, was varied independently showed that less of both spreading and absorption occurred as the droplet viscosity was increased. Furthermore, in each case $d^* = \alpha e^{\beta\zeta}$, where α and β are constants. If the exponent constant (logged), β, is plotted as a function of the viscosity (logged), there is an approximately linearly proportional increase between the two, proving that $\beta = a\mu^b$, where a and b are constants. Therefore, spreading can be related to both the absorption and viscosity as shown in Equation 1.

$$d^* = \alpha e^{\zeta\left(a\mu^b\right)} \quad (1)$$

Topographical irregularity – roughness, spreading and absorption calculations

The surface roughness values, φ, of hemispherical, cubic and plate-like surface profiles were calculated using Equations 2-4, which were derived to include the shape-area influence and the aspect ratio. In these equations, A is the flat plane area (assuming no protrusions), r is the radius of a sphere or solid cylinder, y is a cubic centroid-to-edge distance and h is the protrusion height.

$$\varphi_{halfsphere} = \frac{A - \left(\sum_i \pi r_i^2\right) + \sum_i 2\pi r_i}{A}\left\{\frac{\bar{h}}{\sqrt{\pi \bar{r}^2}}\right\} \quad (2)$$

$$\varphi_{halfcube} = \frac{A - \left(\sum_i 2y_i^2\right) + 3\sum_i 2y_i^2}{A}\left\{\frac{\bar{h}}{\sqrt{2\bar{y}^2}}\right\} \quad (3)$$

$$\varphi_{platelike} = \frac{A - \left(\sum_i \pi r_i^2\right) + \left[\sum_i \left(\pi r_i^2 + h_i\right)\right]}{A}\left\{\frac{\bar{h}}{\sqrt{\pi \bar{r}^2}}\right\} \quad (4)$$

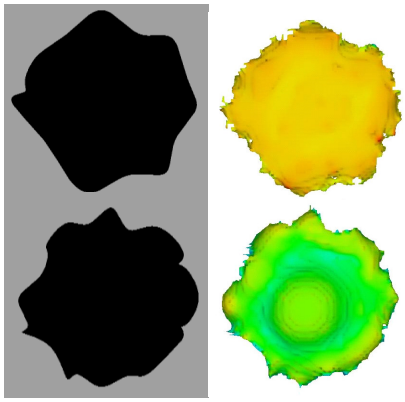

Fig. 1 Examples of mimicked plan view surface spread

Since the topography is irregular, the surface spread was calculated as a plan view surface spread. The plan view surface spread of droplets is calculated by measuring the spreading profile and attributing point locations, the locations are then closed by a series of 3rd order polynomials and integration about local axes yields the plan view spreading area, Figure 1. The absorption is calculated as a volume below the originally flat surface (before protrusions were introduced).

Topographical irregularity – random monodisperse spheres and periodic pyramids

Randomly positioned hemispheres of equal height are studied. The heights studied were 1, 2 and 3μm yielding median surface roughness values of 0.81, 0.84 and 0.90 respectively and median protrusion numbers of 220, 62 and 34 respectively. Figure 2 shows 1st order inverse proportionality between the mean plan view spread plotted as a function of the surface roughness. It is also evident that more frequent smaller protrusions allow greater surface spreading than less frequent higher protrusions. In Figure 3 the mean plan view spread is shown to be linearly proportional to the volume of imbibed fluid. In this case, smaller protrusions also allow more fluid to absorb into the porous substrate than larger ones. Systematic pyramidal structures are generated and taken as homonymous with half spheres. The structures are generated by eroding away solid space at sine and cosine periods along orthogonal Cartesian axes (x and y) respectively, whilst also eroding space at tan periods in the vertical (z) direction. Similarly to the flat surface models, in these simulations, d^* is found to increase exponentially as a function of the maximum absorption depth. Additionally, the magnitude of spreading relative to absorption is higher in smaller height protrusions as it is in larger diameter protrusions.

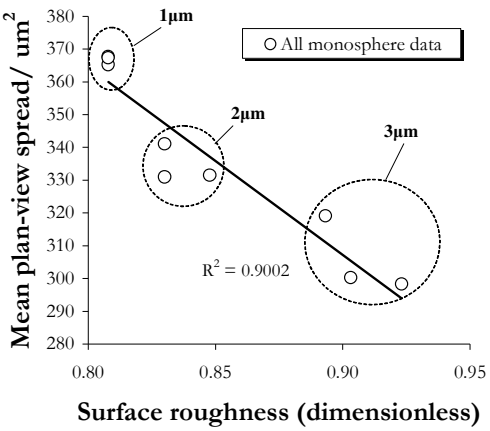

Fig. 2 Spreading plotted against surface roughness

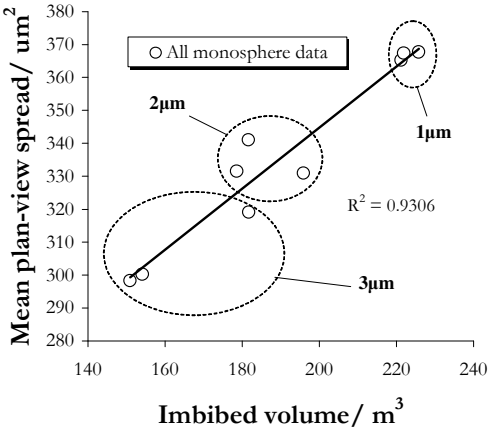

Fig. 3 Spreading plotted against imbibed volume

Topographical irregularity – random polydisperse spheres, cubes and plates

Random polydisperse surfaces using hemispheres, half-cubes and plate-like protrusions were used to assess the effect of size range, frequency and shape on spreading and absorption. For both the hemispherical and half-cube protrusions, the height range was varied between 1-2µm, 1-4µm and 1-6µm. With the plate-like protrusions, the height was kept constant (1µm) but the radius of the plate was varied as 1-2µm, 3-9µm and 3-12µm. Each protrusion (for the half-cubes and plates) was assigned a random value for rotation in each Cartesian axis. The respective median roughness values for the hemispheres were 0.88, 0.91 and 0.93. For the half-cubes, the median values calculated for the roughness were 1.13, 1.48 and 1.52 respectively. The median values for roughness were calculated for the plates as 0.57, 0.14 and 0.13 respectively. One example from each packing showing both the surface spread and inter-protrusion spread is shown in Figure 4.

Figure 5 shows the mean plan view spread plotted as a function of the surface roughness for all the different surfaces. The error bars indicate one standard deviation either side of the arithmetic mean. There appears to be an inverse relationship between the spreading and the surface roughness both; within each group and when comparing between all the groups. However, when comparing between all the groups, it is clear that the scatter is high, much more so than for the monodisperse surface profiles. This is expected as both the locations and sizes of the particles are randomly distributed across the surface. Therefore, as the magnitude of spreading has an aspect ratio dependency, much is reliant on whether larger or smaller protrusions are located in the vicinity of the spreading droplet.

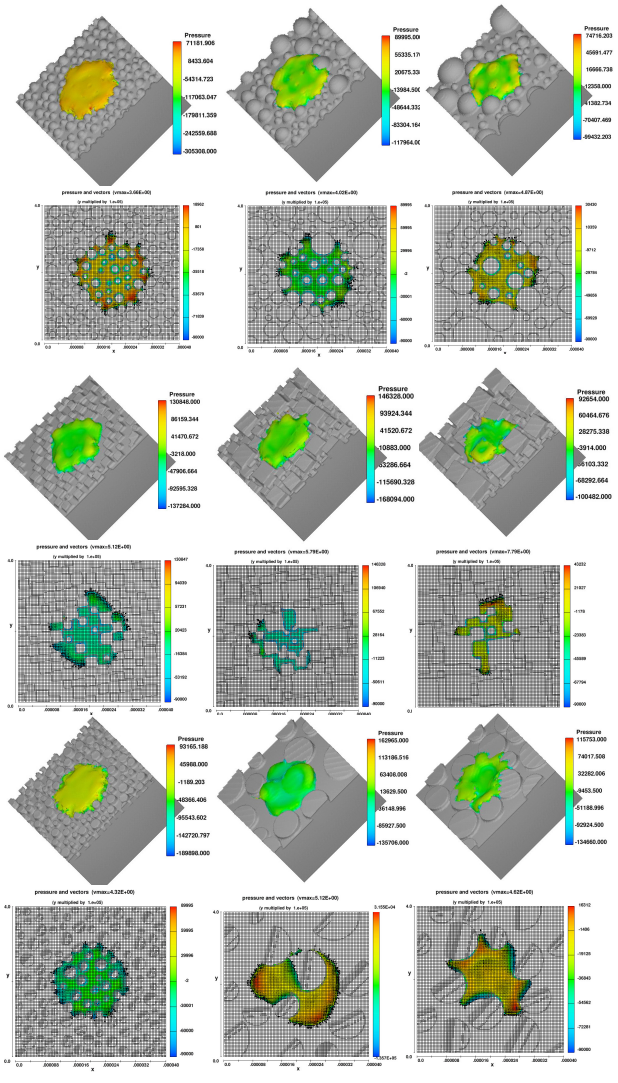

Fig. 4 Spreading profiles for different surfaces

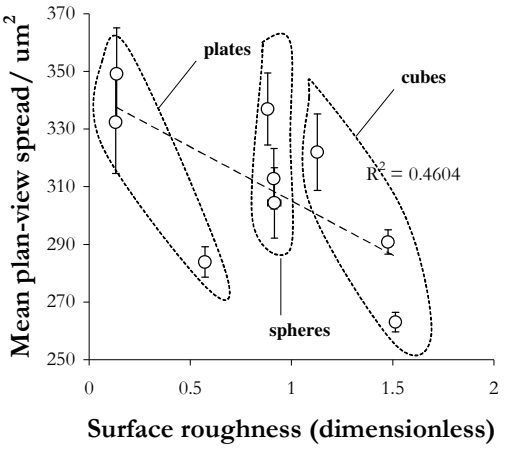

Fig. 5 Spreading plotted against the surface roughness

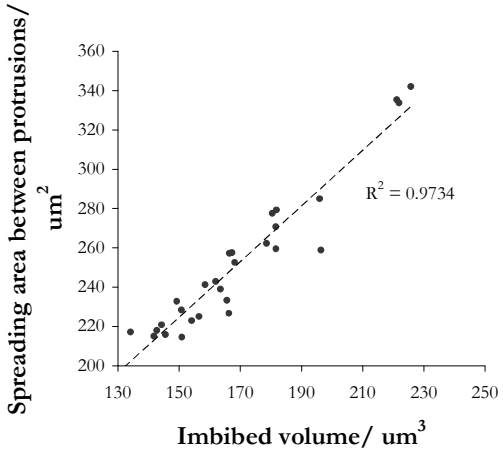

Fig. 6 Spreading plotted against the imbibed volume

The spreading area between the protrusions is plotted in Figure 6 as a function of the volume imbibed into the porous media. There is convincing linear proportionality between the two. The final chart, Figure 7, shows the effect of speed relative to the contact angle on the spreading profile of impacting droplets. In this case, 10µm droplets were used on monodisperse hemispherical surfaces with protrusion heights of 3µm. Contact angles of 30° and 70° were used. Whereas the velocity of the impacting droplet has a noticeable effect on both the plan view spreading and the volume imbibition, the contact angle has little relevance in the 'first phase' of droplet-substrate contact, which is the subject of this study. It is therefore plausible to stipulate that in the early, most dynamical phase of droplet spreading-absorption, pressure driven flow is dominant and contact angle driven flow (wetting flow) is insignificant, even though the droplet sizes are small.

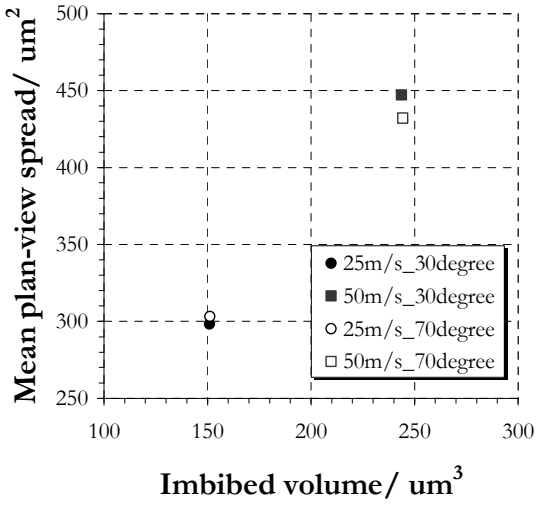

Fig. 7 Contact angle-impaction effects

Conclusions

- For both flat and periodically irregular surface profiles, the spreading (d* or plan view) is an exponential function of the maximum absorption depth.
- It has been shown that $d^* = \alpha e^{\zeta(a\mu^b)}$ for flat surfaces.
- Equations have been derived to calculate roughness as a dimensionless product of the normalised surface area and the shape-related aspect ratios of surface protrusions.
- Half-cubes generate rougher surfaces than hemispheres, which yield higher values for roughness than plates.
- Plan view spreading is a linear function of imbibition but is inversely proportional to the surface roughness.
- Inter-protrusion spreading shows 1st order proportionality with the volume imbibition.
- At high impact velocities, pressure driven flow is dominant and contact angle driven flow is insignificant.

References

[1] Raiskinmäki, P., Koponen, A., Merikoski, J. and Timonen, J. (2000); Spreading dynamics of three-dimensional droplets by the lattice-Boltzmann method; Computational Materials Science 18, 7-12.

[2] Dubé, M., Chabot, B., Daneault, C. and Alava, M. (2005); Fundamentals of fluid front roughening in imbibition; Pulp and Paper Canada 106:9, 178-182.